

## PHYSICAL CONDITIONS IN REGIONS OF LINE FORMATION OF SOLAR TYPE STARS

L. H. Rodrigues-Merino<sup>1</sup>, O. Cardona<sup>1</sup>, and A. Flores<sup>2</sup>

*We present the physical parameters of the regions with spectral line formation of a set of stars classified as G2. The method employed in this analysis only requires the full width at half maximum of each spectral line, the effective temperature of the star, and few basic atomic parameters. The physical parameters estimated in this work are compared with results obtained with stellar atmosphere models.*

Keywords: *line: formation (Physical conditions); stars: solar-type*

### 1. Introduction

Solar type stars play an important role in the search for life. Currently there are several instruments in operation with the main goal to look for planets located in habitable zones (e.g., The Kepler Mission). This type of star presents the optimal conditions for sustaining life because of the low ultraviolet emission; therefore, it is mandatory to understand as well as possible the physics of their atmospheres.

Several astrophysical groups have developed numerical codes to model both the stellar atmospheres and the line profile spectra. In some cases codes and results are available to the astronomical community, like Atlas9 and

---

<sup>1</sup> Instituto Nacional de Astrofísica, Óptica y Electrónica, Tonantzintla, Puebla, México, e-mail: lino@inaoep.mx

<sup>2</sup> Facultad de Ingeniería, Universidad Autónoma del Carmen, Ciudad del Carmen, México, e-mail: aflores@pampano.unacar.mx

Synthe codes built by Kurucz [1,2]<sup>1</sup> or TLUSTY and SYNSPEC codes built by Hubeny & Lanz [3]<sup>2</sup>. The numerical codes compute the atmosphere models based on different arguments: local thermodynamic equilibrium (LTE), and non local thermodynamic equilibrium (NLTE), plane parallel atmospheres, spherical atmospheres, etc. Once a stellar atmosphere model has been computed, it is possible to calculate the spectral energy distribution emitted by the atmosphere model, and within the process of computing the atmosphere model and the spectrum, it is feasible to follow the change of some physical parameters as function of the physical depth in the atmosphere.

In order to find out an alternative procedure to make a diagnostics of the physical conditions of regions in stellar atmosphere where spectral lines are being formed, Cardona [4] has performed a statistical mechanics analysis of the atomic line broadening by thermal energy fluctuations in a gaseous system. He found that the width of an atomic spectral line is strongly correlated with the physical conditions of the line forming region. The physical parameters associated with the full width at half maximum (fwhm) of a spectroscopic line are the temperature, the number density of particles, and the principal quantum numbers related with the transition that produces the line. Based on this method, Cardona et al. [5] have performed an analysis of the region in the atmosphere of two stars, the white dwarf star G191-B2B and the variable star V803-Cen, where the Lyman- $\zeta$  line is being formed. Their conclusions were compared with the results of atmosphere models.

Now using the equations obtained by Cardona [4] we determined the physical conditions of regions in the atmosphere of solar type stars where the Balmer and magnesium lines are being formed. In order to be more confident with the parameters estimated in this study, we performed a comparison with the results of the solar atmosphere model. The paper is organized as follows: In Section 2 we present the theoretical arguments employed to infer the physical properties of the regions with spectral line formation. In Section 3, we describe the observational data used in this work. The method followed to measure the fwhm of the selected spectral lines and the results are described in Section 4. In Section 5 we perform a comparison between the newly determined properties and results obtained with the computation of a stellar atmosphere model. The use of the fwhm of an atomic spectral line as a tool to determine physical properties of the stellar atmosphere is discussed in Section 6.

## 2. Broadening of spectral lines

The spectral lines of an isolated atom are, in principle, nearly perfectly sharp; however, due to the finite lifetime of the energy levels, the lines are naturally broadened. The spectral energy distribution emitted by the plasma of a stellar atmosphere is plagued with several absorption lines. The profile of any spectroscopic line is fully related with the physical properties of the forming region. The traditional approach employed to model the profile of the spectral lines is based on considering that there are, basically, three processes that broaden the spectroscopic lines; (1) the natural broadening which is produced by the interaction of the light with the atoms, (2) the pressure broadening, which is essentially caused by the collisions between atoms, and (3) the thermal broadening, which arises

---

<sup>1</sup> <http://kurucz.harvard.edu/>

<sup>2</sup> <http://nova.astro.umd.edu/>

because of the velocity distribution of the ensemble of atoms. The broadening of the spectroscopic lines produced by any of the processes quoted above is usually described by the absorption coefficient per atom ( $\alpha$ ). The combined result of the different processes is given by the convolution of all the absorption coefficients,

$$\alpha(\text{total}) = \alpha(\text{natural}) \cdot \alpha(\text{pressure}) \cdot \alpha(\text{thermal}). \quad (1)$$

The absorption coefficients of the natural and pressure broadening are described by Lorentzian profiles; meanwhile the absorption coefficient of the thermal broadening has a Gaussian profile, and the convolution of these profiles results in a new profile, the Voigt profile.

An alternative method developed to understand the broadening of the spectroscopic lines was introduced by Cardona [4]. He based his study on the analysis of the energy fluctuations of a thermodynamic system. The energy fluctuations of a system can be produced by several kinds of processes, like the collisions between particles of the ensemble; therefore this alternative analysis must provide us with equations that describe very closely the broadening of spectral lines. The equations given by Cardona [4] (Eqs. (14) and (16) in his work) relate the full width at half maximum of the spectroscopic lines of hydrogenic and nonhydrogenic atoms (respectively) with the physical conditions of the line-forming region, and with few basic atomic parameters; obviously some mechanisms of line broadening, like the stellar rotation or the instrumental effects, are not considered by these equations. Although in all stellar spectra most of the spectral lines are in absorption, it is very common to find the line width at half height denoted as the full width at half maximum.

The main difference between the two methods given above is that the first method describes the broadening of spectroscopic lines as a function of thermodynamic quantities and quantum mechanical parameters (not easy to determine), and the second method describes the broadening of spectral lines mostly based on thermodynamic quantities. Therefore, the equation based on the analysis of energy fluctuations can be used to explore the physical properties of the line forming regions (see Cardona et al. [5]).

### 3. Observational Data

We have performed the analysis of several absorption lines that are important features in the spectrum of a solar type star. The selected lines are four Balmer lines ( $H\alpha$ ,  $H\beta$ ,  $H\gamma$  and  $H\delta$ ), and the lines of the magnesium triplet (Mgb1, Mgb2, and Mgb3). The set of spectra used to study the regions of line formation was retrieved from the ELODIE library V3.1<sup>3</sup> through Hyper-Leda database<sup>4</sup>. The archive hosts around two thousand spectra, and it covers the whole spectral type range. The wavelength range covered by any spectrum of the ELODIE Library spans from around 3900Å to 6800Å (see Prugniel and Soubiran [6]; Prugniel et al. [7]). It is possible to retrieve fluxes at two resolutions ( $R = 42000$  and  $R = 10000$ ); in the case of the spectra at high resolution, the fluxes are normalized to

<sup>3</sup> <http://www.obs.u-bordeaux1.fr/m2a/soubiran/elodielibrary.html>

<sup>4</sup> <http://leda.univ-lyon1.fr/11/spectrophotometry.html>

TABLE 1. List of Stars Employed to Measure the FWHM of the Selected Spectral Lines. Fits Files Obtained from ELODIE Library Provided the Stellar Atmosphere Parameters

| Star      | Spectral type<br>ELODIE | Spectral type<br>SIMBAD | $T_{eff}$<br>K | logg | [Fe/H] | $v \sin i$<br>km/s |
|-----------|-------------------------|-------------------------|----------------|------|--------|--------------------|
| Sun       |                         | G2 V                    | 5777           | 4.44 | +0.00  | 2.0                |
| HD 245    | G2 V                    | G2 V                    | 5772           | 4.15 | -0.59  | 3.0                |
| HD 3628   | G2 V                    | G2 V Va.                | 5699           | 4.02 | -0.18  | 1.0                |
| HD 4307   | G2 V                    | G0 V                    | 5744           | 3.85 | -0.29  | 2.0                |
| HD 9562   | G2 IV                   | G1 V                    | 5777           | 3.85 | +0.125 | 4.0                |
| HD 10307  | G2 V                    | G1.5 V                  | 5793           | 4.11 | -0.02  | 3.0                |
| HD 12235  | G2 IV                   | G2 IV                   | 5858           | 3.89 | +0.180 | 5.0                |
| HD 12846  | G2 V                    | G2 V                    | 5727           | 4.41 | -0.25  | 2.0                |
| HD 14802  | G2 V                    | G1 V                    | 5830           | 3.89 | -0.06  | 4.0                |
| HD 23050  | G2 V                    | G2 V                    | 5772           | 4.04 | -0.43  | 3.0                |
| HD 76752  | G2 V                    | G2 V                    | 5708           | 4.23 | +0.00  | 2.0                |
| HD 81809  | G2 V                    | G5 VFe-1CH-0.8          | 5610           | 3.83 | -0.36  | 1.8                |
| HD 84737  | G2 V                    | G0.5 Va                 | 5768           | 3.89 | +0.096 | 2.3                |
| HD 89010  | G2 IV                   | G1.5 IV-V               | 5669           | 3.84 | -0.01  | 3.5                |
| HD 105546 | G2 III                  | G2 IIIw                 | 5016           | 2.21 | -1.58  | 5.2                |
| HD 119550 | G2 V                    | G2 V                    | 5723           | 3.83 | -0.09  | 4.0                |
| HD 126868 | G2 III                  | G2 IV                   | 5778           | 3.81 | -0.02  | 14.3               |
| HD 137107 | G2 V                    | G0 V                    | 5919           | 4.21 | -0.11  | 5.3                |
| HD 143761 | G2 V                    | G0 V                    | 5749           | 4.02 | -0.26  | 4.0                |
| HD 159181 | G2 II                   | G2 Iab:                 | 5368           | 1.22 | -0.13  | 11.6               |
| HD 168009 | G2 V                    | G2 V                    | 5728           | 4.14 | -0.04  | 3.0                |
| HD 186408 | G2 V                    | G1.5 Vb                 | 5732           | 4.10 | +0.108 | 4.0                |
| HD 209750 | G2 Ib                   | G2 Ib                   | 5399           | 0.95 | -0.06  | 7.9                |
| HD 221170 | G2 IV                   | G2 IV Va                | 4561           | 1.10 | -2.10  | 7.4                |
| HD 225239 | G2 V                    | G2 V                    | 5590           | 3.75 | -0.47  | 2.0                |

the pseudo-continuum. In order to avoid as much as possible the effects of spectral line blending, we have decided to use the spectral energy distributions at high resolution; therefore we have selected the normalized flux of 24 solar type stars. We also have used the Solar Flux Atlas (Kurucz et al. [8]) retrieved from the Kurucz web page, which includes the optical part of the solar spectrum measured at high resolution. Table 1 shows the stars classified as G2 in the ELODIE library, it also provides the spectral type, the luminosity class (according to ELODIE library and

SIMBAD database), the atmospheric parameters (effective temperature, surface gravity, and metallicity), and the rotational velocity. The atmosphere parameters of the stars from ELODIE library have been retrieved from the FITS file of each spectrum (the set of atmospheric parameters used was determined based on internal comparisons within the library), and the rotational velocity values are reported by Glebocki and Gnacinski [9].

#### 4. Analysis of the Line-Forming Regions

All the physical properties imprinted in the spectral energy distribution (SED) emitted by a star are due to physical processes produced in the stellar atmosphere. The continuum arises from regions of the stellar atmosphere where the Rosseland optical depth is  $\tau_{ross} = 2/3$ ; in this part of the atmosphere the temperature is equal to the

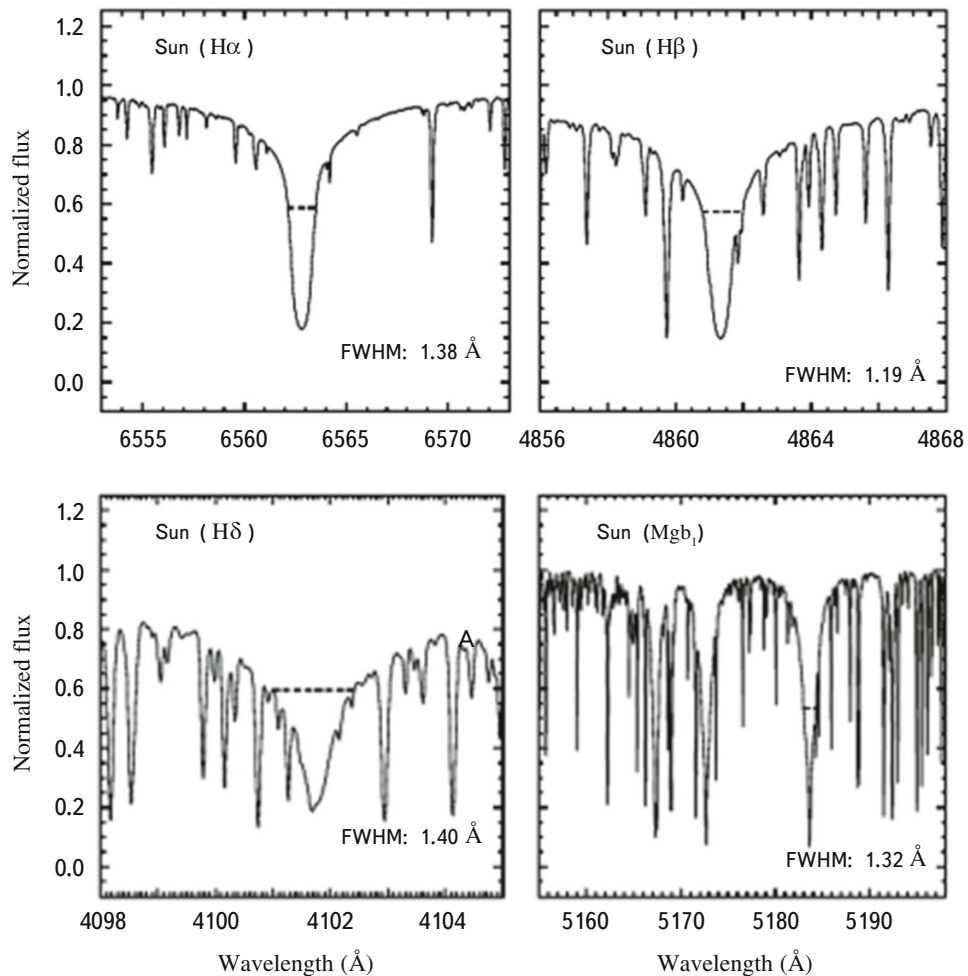


Fig.1. The panels display the spectral energy distribution of the Sun around four absorption features; H $\alpha$ , H $\beta$ , H $\delta$ , and Mgb<sub>1</sub>. The full width at half maximum of each spectral line is displayed with a discontinuous line, and its value is shown on the right lower part of each panel.

effective temperature. Meanwhile absorption lines of the SED are being formed in regions located between the continuum forming region and the top of the atmosphere. Cardona [4] found that the full width at half maximum of an atomic spectral line is given by

$$w = \frac{2\pi a_0}{3\alpha Z_{eff}} kT \sqrt[3]{N} (n_{i,eff}^2 + n_{f,eff}^2), \quad (2)$$

where  $N$  and  $T$  are physical parameters of the region of line formation;  $N$  is the number density of particles,  $T$  is the temperature,  $n_{i,eff}$  and  $n_{f,eff}$  are the effective principal atomic quantum numbers of the levels producing the line,  $Z_{eff}$  is the effective charge of the atom,  $k$  and  $a_0$  are the Boltzmann constant and the Bohr radius, respectively, and  $\alpha$  is a numerical constant. In order to explore the physical conditions of the regions where the selected spectroscopic lines are being formed, we measured the full width at half maximum of the spectral lines.

The selected lines produce prominent absorption features in the spectrum of a solar type star; therefore they played important roles in several works, e.g., see Worthey and Ottaviani [10] and Worthey et al. [11]. According to

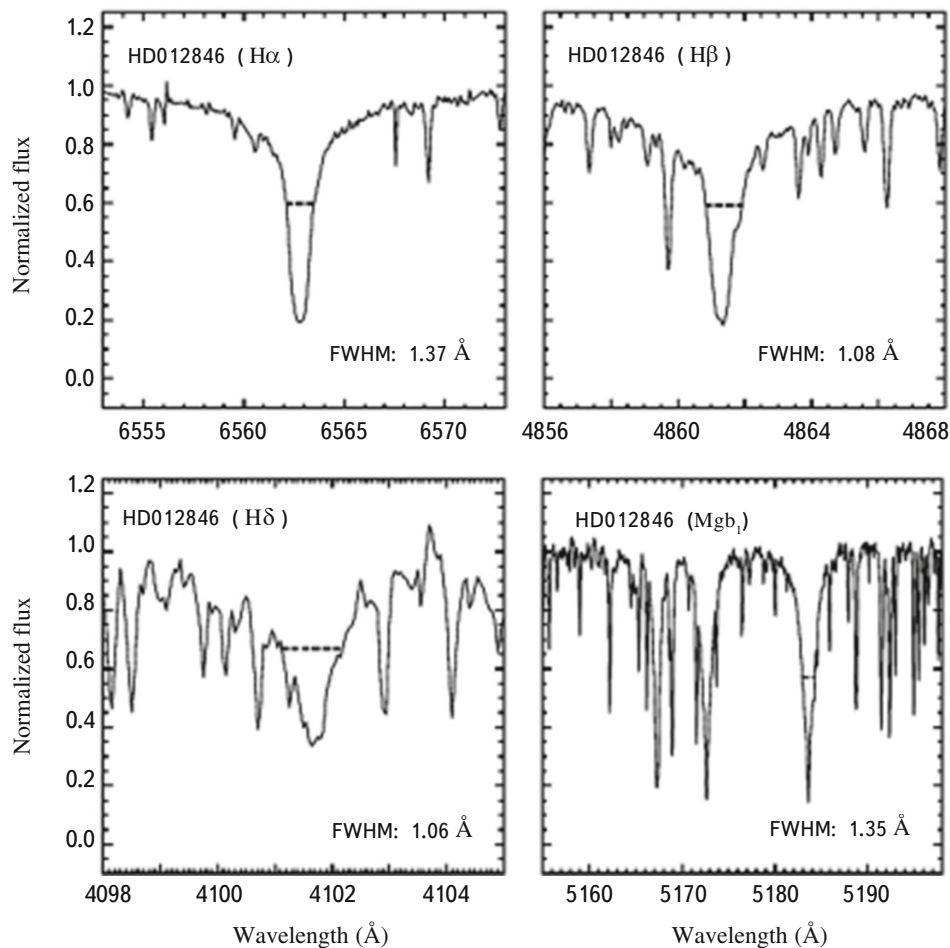


Fig.2. Similar to Fig.1, in this case the star is HD 12846.

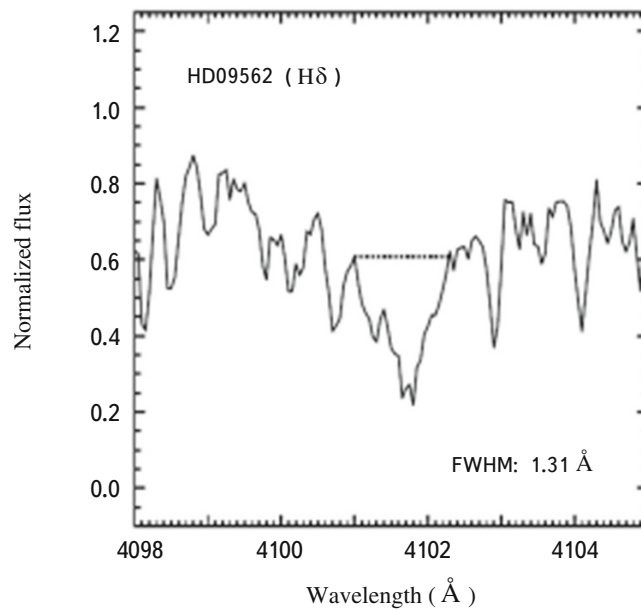


Fig.3. In a few cases, the spectral line blending does not allow us to measure the fwhm of the selected spectral line. The spectral region close to the H $\delta$  line of the HD 9562 star is populated by several spectral lines, making difficult the measurement of the fwhm of this line.

ELODIE library, all the chosen stars are assigned a G2 spectral type classification, most of them are identified as dwarfs, and only few stars are classified as giants or super-giants. However, according to the SIMBAD database, there are some stars that are not classified as a G2 spectral type star (see Table 1), and thus one has to keep in mind that there could be some stars that are misclassified. Stars with different luminosity classes from our selected set of spectra will allow us to explore regions under different physical conditions.

The shape of the absorption line is known as the Voigt profile, which is the result of the convolution of Gaussian and Lorentzian profiles (see Section 2). In order to measure the width of a selected spectral feature at the half maximum, we performed a linear interpolation of the spectral energy distribution around the minimum of the selected line. The interpolation used a wavelength step of around 0.001Å. Because we have employed the normalized spectra of the ELODIE library, we only had to measure the width of the interpolated line at the middle distance between the minimum of the flux and the unit. Figures 1 and 2 display parts of the spectrum of the Sun and the star HD 12846, showing the H $\alpha$ , H $\beta$ , H $\delta$ , and the magnesium lines. The discontinuous line in each panel describes the full width of the spectroscopic line at half of the maximum. The fwhm measured is given at the right lower part of each panel. Although we have used a set of spectra with high spectral resolution, we could not avoid completely the effects of line blending in all the measurements of the fwhm. Figure 3 shows that the spectral region close to the H $\delta$  line of the star HD 9562 is populated by several spectral lines, which makes difficult to measure the fwhm of this Balmer line.

The files with normalized fluxes of the ELODIE library do not provide the errors of the stellar fluxes. In order to estimate the error in the measurement of the width of a spectroscopic line, we have followed a Monte Carlo method. We have selected a spectrum, and we have generated randomly several similar spectra. We used the RMS of the selected spectrum to generate the set of spectra. Using the generated spectra we obtained a set of widths of the same spectroscopic line. A simple statistical analysis allowed us to determine that the error in the measurement of the fwhm of any spectral line is negligible. Table 2 gives the value of the fwhm of all selected spectral lines. In three cases, HD 9562 (H $\delta$ ), HD 159181 (H $\gamma$ ), and HD 209750 (H $\gamma$ ), it was not possible to measure the width of the line due to problems with the line blending, and in the case of the star HD 76752 (H $\delta$ ) the spectrum shows an emission line in the region of the selected spectral feature.

TABLE 2. FWHM (in  $\text{\AA}$ ) of the Selected Spectral Lines of the Sun and G2-Type Stars. In Four Cases, it was not Possible to Measure the Width of the Line (see the text)

| Star      | H $\alpha$ | H $\beta$ | H $\gamma$ | H $\delta$ | Mgb3 | Mgb2 | Mgb1 |
|-----------|------------|-----------|------------|------------|------|------|------|
| Sun       | 1.38       | 1.19      | 1.21       | 1.40       | 0.71 | 0.96 | 1.32 |
| HD 245    | 1.44       | 1.09      | 1.03       | 1.11       | 0.56 | 0.75 | 0.94 |
| HD 3628   | 1.36       | 1.10      | 1.02       | 1.08       | 0.60 | 0.86 | 1.25 |
| HD 4307   | 1.50       | 1.13      | 0.96       | 1.06       | 0.52 | 0.66 | 0.80 |
| HD 9562   | 1.41       | 1.20      | 1.11       | -          | 0.60 | 0.78 | 1.18 |
| HD 10307  | 1.49       | 1.19      | 1.11       | 1.35       | 0.63 | 0.83 | 1.23 |
| HD 12235  | 1.54       | 1.27      | 1.20       | 1.34       | 0.60 | 0.77 | 1.18 |
| HD 12846  | 1.37       | 1.08      | 0.99       | 1.06       | 0.69 | 1.00 | 1.35 |
| HD 14802  | 1.47       | 1.20      | 1.20       | 1.11       | 0.55 | 0.65 | 0.86 |
| HD 23050  | 1.40       | 1.10      | 1.01       | 1.11       | 0.54 | 0.73 | 0.94 |
| HD 76752  | 1.33       | 1.08      | 1.04       | -          | 0.72 | 0.95 | 1.34 |
| HD 81809  | 1.43       | 1.08      | 0.97       | 1.20       | 0.64 | 0.88 | 1.22 |
| HD 84737  | 1.52       | 1.18      | 1.13       | 1.20       | 0.59 | 0.77 | 1.11 |
| HD 89010  | 1.49       | 1.15      | 1.01       | 1.21       | 0.61 | 0.78 | 1.19 |
| HD 105546 | 1.44       | 0.94      | 0.78       | 0.78       | 0.40 | 0.34 | 0.40 |
| HD 119550 | 1.48       | 1.14      | 0.99       | 1.05       | 0.55 | 0.67 | 0.97 |
| HD 126868 | 1.85       | 1.25      | 1.03       | 1.07       | 0.67 | 0.79 | 1.12 |
| HD 137107 | 1.52       | 1.29      | 1.14       | 1.24       | 0.58 | 0.73 | 1.07 |
| HD 143761 | 1.42       | 1.08      | 1.04       | 1.29       | 0.59 | 0.77 | 1.02 |
| HD 159181 | 2.84       | 1.88      | -          | 1.22       | 0.71 | 0.77 | 1.18 |
| HD 168009 | 1.36       | 1.15      | 1.05       | 1.25       | 0.66 | 0.90 | 1.28 |
| HD 186408 | 1.38       | 1.19      | 1.08       | 1.24       | 0.69 | 0.94 | 1.31 |
| HD 209750 | 2.49       | 1.64      | -          | 1.11       | 0.69 | 0.71 | 1.14 |
| HD 221170 | 1.40       | 0.93      | 0.72       | 0.64       | 0.39 | 0.32 | 0.37 |
| HD 225239 | 1.43       | 1.02      | 0.87       | 1.10       | 0.52 | 0.63 | 0.79 |



Figure 4 displays the values of fwhm of the selected spectral lines. The set of values of the fwhm of each spectral line spans around a common value. The giant and super-giant stars (diamond, triangle and square, respectively) depart from the trend followed by most of the stars because they present stronger Balmer lines. On the other hand, stars HD 105546 and HD 221170 (the most metal-poor stars of the set) display thinner spectral lines than the common values, in particular their magnesium lines. These departures from the mean values are produced by particular physical phenomena, whose study is outside the scope of this work.

We used Eq. (2) and the full width at half maximum of each selected spectral line to estimate the density of particles of the region where the line is being formed. Figure 5 displays, according to Eq. (2), the change of the fwhm of the  $H\alpha$  line as a function of the number density of particles and temperature (stated lines); we employed five temperatures: 100, 90, 80, 70, and 60% of the effective temperature of the Sun; the horizontal line correspond to the fwhm of the  $H\alpha$  line measured in the solar spectrum. This plot allows us to infer the density of particles of the region in the solar atmosphere where the  $H\alpha$  line is being formed. Cardona et al. [5] have shown that the Balmer lines as well as the magnesium lines are formed in a region of the stellar atmosphere where the temperature is close to 80% of the effective temperature; therefore we have employed Eq. (2), three temperatures (85, 80, and 75% of the effective temperature of each star), and the full width at half maximum of the selected spectral lines to determine the number density of particles in the regions where the spectroscopic lines are being formed. Table 3 gives the number density of particles of the regions where each selected spectral line is being formed. The density of particles of the region where the  $H\alpha$  line is being formed has a common value of  $N \sim 12 \times 10^{15}$  particles  $\text{cm}^{-3}$ . There are four stars (HD 126868, HD 159181, HD 209750, and HD 221170), in which the number density of particles estimated is larger than

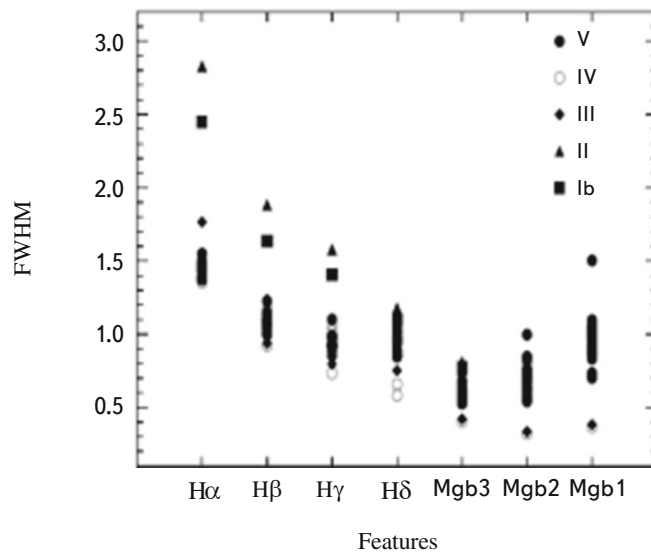


Fig.4. The fwhms of each selected spectral line are distributed around a common value. Two special cases are; the Balmer lines, which are formed in the outer parts of the atmosphere, of giant stars are wider, while the magnesium lines of the metal poor stars are thinner (see the text).

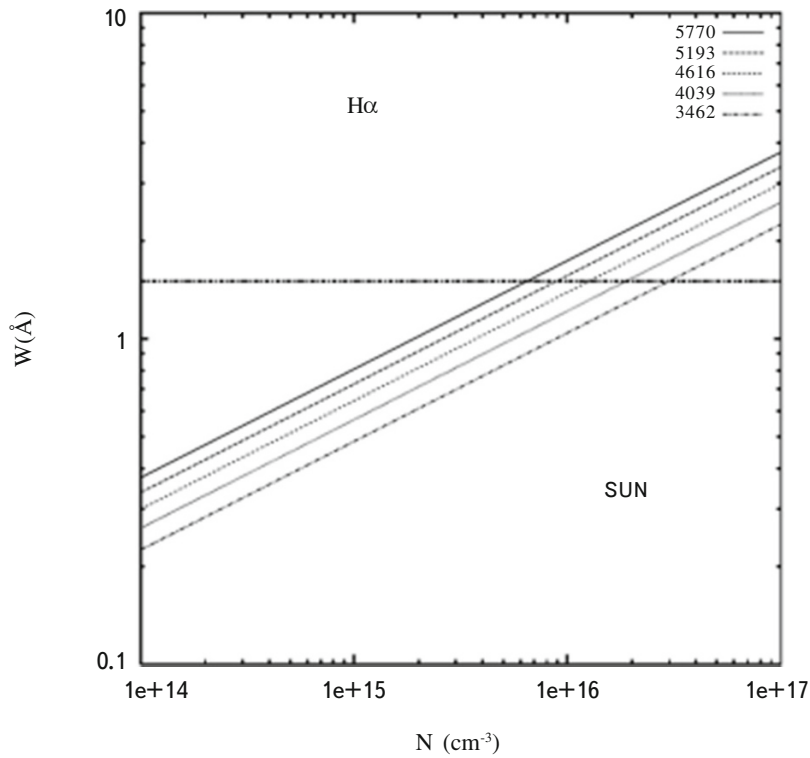


Fig.5. The full width at half maximum of the  $H\alpha$  line as function of the particle density. The started lines correspond to percentages of the effective temperature (100, 90, 80, 70 and 60%) of the Sun. The horizontal line shows the width of the  $H\alpha$  line measured using the Solar Flux Atlas (Kurucz et al. [8]). The number density of particles where the  $H\alpha$  line of the Sun is being formed is around  $1 \times 10^{16}$  particles  $\text{cm}^{-3}$ .

the common value, the reason could be that they are fast rotators, hence their spectroscopic lines are strongly affected by the rotation. The  $H\beta$  absorption lines are less affected by the rotation, and the rest of the analyzed Balmer lines do not depart from the respective common value. Also it is important to note that the magnesium lines are good tracers of metallicity, and the stars HD 105546 and HD 221170 have the lowest chemical abundances (see Table 1); and this is probably the reason why the number densities of their line-forming regions have the lowest values.

## 5. Comparisons

In order to show that the results obtained with Eq. (2) are in accord with physical properties of the stellar atmospheres of G2-type stars, we decided to compare these results with physical parameters of the solar atmosphere model. The atmosphere model allows us to know several parameters, like the particle density ( $N$ ), the temperature ( $T$ ), the pressure ( $P$ ), etc., as function of the geometrical depth (Rosseland optical depth,  $\tau_{ross}$ ) inside the atmosphere.

TABLE 3. Number Density of Particles ( $\times 10^{15}$  particles  $\text{cm}^{-3}$ ) of the Regions where the Absorption Lines are Being Formed

| Star      | $N(\text{H}\alpha)$ | $N(\text{H}\beta)$ | $N(\text{H}\gamma)$ | $N(\text{H}\delta)$ | $N(\text{Mgb}3)$ | $N(\text{Mgb}2)$ | $N(\text{Mgb}1)$ |
|-----------|---------------------|--------------------|---------------------|---------------------|------------------|------------------|------------------|
| Sun       | 9.96±3.49           | 10.89±4.17         | 7.23±1.84           | 6.12±1.32           | 24.77±21.59      | 25.84±23.45      | 64.10±144.50     |
| HD 245    | 11.30±4.48          | 8.15±2.33          | 4.45±0.70           | 2.98±0.31           | 11.64±4.76       | 11.93±4.99       | 23.13±18.80      |
| HD 3628   | 9.89±3.44           | 8.70±2.67          | 4.49±0.71           | 2.33±0.19           | 14.88±7.80       | 18.69±12.28      | 56.50±112.20     |
| HD 4307   | 12.96±5.91          | 9.21±2.99          | 3.66±0.47           | 2.63±0.24           | 9.46±3.14        | 8.25±2.39        | 14.46±7.35       |
| HD 9562   | 10.59±3.95          | 10.85±4.14         | 5.56±1.09           | 4.89±0.84           | 14.28±7.19       | 13.39±6.28       | 45.63±73.14      |
| HD 10307  | 12.39±5.39          | 10.49±3.86         | 5.51±1.07           | 5.31±0.99           | 16.40±9.44       | 16.00±8.99       | 51.25±92.35      |
| HD 12235  | 13.22±6.13          | 12.33±5.34         | 6.73±1.59           | 5.02±0.88           | 13.69±6.59       | 12.34±5.36       | 43.74±67.26      |
| HD 12846  | 9.97±3.50           | 8.12±2.31          | 4.05±0.58           | 2.66±0.25           | 22.30±17.48      | 28.95±29.47      | 70.13±172.89     |
| HD 14802  | 11.67±4.78          | 10.55±3.92         | 6.83±1.64           | 2.89±0.29           | 10.71±4.03       | 7.54±2.00        | 17.19±10.36      |
| HD 23050  | 10.39±3.79          | 8.38±2.47          | 4.20±0.62           | 2.98±0.31           | 10.44±3.83       | 11.00±4.24       | 23.13±18.80      |
| HD 76752  | 9.21±2.98           | 8.20±2.36          | 4.74±0.79           | 3.08±0.33           | 25.59±23.01      | 25.07±22.06      | 69.27±168.70     |
| HD 81809  | 12.05±5.10          | 8.64±2.63          | 4.05±0.58           | 4.10±0.59           | 18.93±12.60      | 20.99±15.49      | 55.06±106.64     |
| HD 84737  | 13.32±6.26          | 10.36±3.78         | 5.89±1.22           | 3.77±0.50           | 13.64±6.54       | 12.94±5.89       | 38.16±51.18      |
| HD 89010  | 13.22±6.13          | 10.10±3.59         | 4.43±0.69           | 4.08±0.58           | 15.89±8.87       | 14.17±7.03       | 49.52±86.20      |
| HD 105546 | 17.23±10.42         | 7.96±2.23          | 2.95±0.31           | 1.58±0.09           | 6.47±1.47        | 1.69±0.10        | 2.71±0.26        |
| HD 119550 | 12.59±5.58          | 9.57±3.22          | 4.06±0.58           | 2.59±0.24           | 11.32±4.50       | 8.73±2.68        | 26.07±23.89      |
| HD 126868 | 23.89±20.09         | 12.25±5.27         | 4.44±0.69           | 2.66±0.25           | 19.88±13.91      | 13.90±6.80       | 38.99±53.49      |
| HD 137107 | 12.33±5.34          | 12.53±5.53         | 5.60±1.10           | 3.85±0.52           | 11.99±5.05       | 10.20±3.66       | 31.63±35.17      |
| HD 143761 | 10.97±4.24          | 8.02±2.26          | 4.64±0.76           | 4.74±0.79           | 13.78±6.66       | 13.06±6.01       | 29.90±31.47      |
| HD 159181 | 107.79±408.77       | 51.99±94.97        | 5.70±1.14           | 4.92±0.85           | 29.50±30.63      | 16.05±9.08       | 56.87±113.69     |
| HD 168009 | 9.74±3.33           | 9.79±3.37          | 4.83±0.82           | 4.36±0.67           | 19.50±13.36      | 21.09±15.64      | 59.75±125.41     |
| HD 186408 | 10.16±3.63          | 10.83±4.13         | 5.24±0.97           | 4.24±0.63           | 22.24±17.40      | 23.99±20.22      | 63.91±143.66     |
| HD 209750 | 71.41±179.28        | 37.11±48.41        | 6.27±1.38           | 3.64±0.47           | 26.61±24.93      | 12.37±5.39       | 50.40±89.29      |
| HD 221170 | 21.05±15.57         | 10.26±3.71         | 3.08±0.33           | 1.16±0.05           | 7.97±2.23        | 1.88±0.12        | 2.86±0.29        |
| HD 225239 | 12.19±5.22          | 7.35±1.90          | 2.95±0.31           | 3.19±0.36           | 10.26±3.70       | 7.78±2.13        | 15.11±8.05       |

It is important to keep in mind that a stellar atmosphere model provides information that describes approximately the formation of spectral lines (see Cardona et al. [5]); however, it can be a good benchmark. We decided to calculate the solar atmosphere model using the code developed by Crivellari et al. [12]. The effective temperature used to compute the solar model was 5770 K, the logarithm of the surface gravity was 4.44 dex, and the model has been calculated using the solar abundance. The spectral lines are being formed in regions with  $\tau_\nu = 1$ . Figure 6 shows the Rosseland optical depth as a function of the frequency. The model allows us to determine that in the solar atmosphere the  $\text{H}\alpha$  absorption line is being formed around a region where the Rosseland optical depth is  $\sim 2.42 \times 10^{-2}$ . At this optical depth the temperature is  $\sim 4600$  K and the pressure is  $\sim 4800$  dy  $\text{cm}^{-2}$ ; therefore the density of particles is around

$7 \times 10^{15}$  particles  $\text{cm}^{-3}$ . The number density of particles obtained with Eq. (2) is  $9.96 \pm 3.49 \times 10^{15}$  particles  $\text{cm}^{-3}$ , which is very close to the previous result. On the other hand, the atmosphere model lets us know that the  $\text{H}\delta$  absorption line is being formed in a region where the optical depth is around  $2.23 \times 10^{-1}$ . At this depth the temperature is  $\sim 5300$  K and the pressure is  $\sim 68000$  dy  $\text{cm}^{-2}$ ; therefore the density of particles is  $\sim 90 \times 10^{15}$  particles  $\text{cm}^{-3}$ . Using Eq. (2) we have obtained that the number density of particles is  $6.12 \pm 1.32 \times 10^{15}$  particles  $\text{cm}^{-3}$ , which is lower than the previous result. It is important to keep in mind two points; first, the atmosphere model describes approximately the formation of spectral lines; then we do not expect to find a very close match between both results. Second, the  $\text{H}\alpha$  absorption line is formed in outer regions of the atmosphere where the temperature is lower, thus large amounts of hydrogen are capable of performing a transition from state  $n = 2$  to the state  $n = 3$ . The  $\text{H}\delta$  line is formed in regions at higher temperatures; thus, there should not be large amounts of hydrogen capable of performing a transition from state  $n = 2$  to state  $n = 6$ .

## 6. Discussion and Conclusions

We have used 25 spectra of stars classified as G2 spectral type in the ELODIE library and the spectrum of the Sun to measure the full width at half maximum of a set of absorption lines. Most of the stars are dwarfs. The set of measurements of each selected spectral feature ranges around a common value. In the case of the Balmer lines,

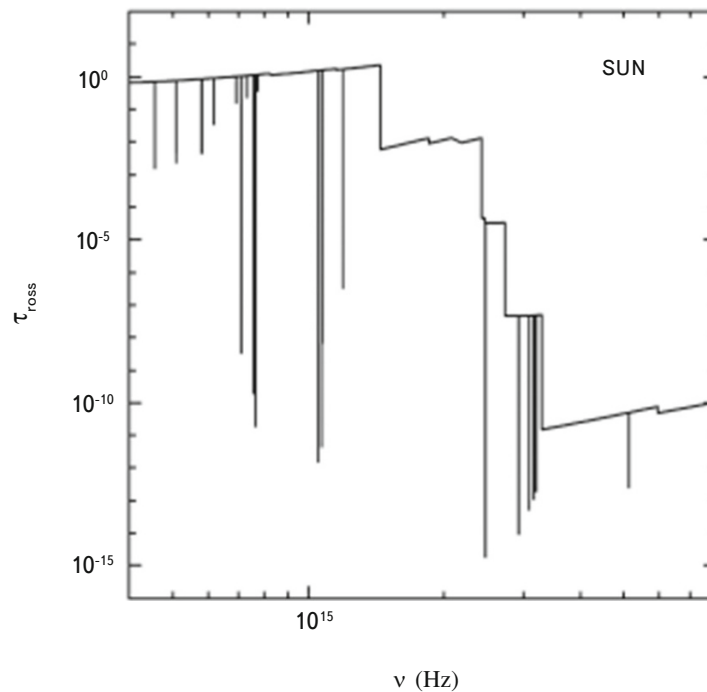


Fig.6. The Rosseland optical depth ( $\tau_{\text{ross}}$ ) as a function of the frequency given by the solar atmosphere model.

we found four stars whose fwhm departs from the common values because they are rapid rotators. We also analyzed two stars that show magnesium lines thinner than the common values, the most likely reason being that these stars are metal poor. The small spread of the fwhms around the common values could be due to the spectral misclassification of some stars, blending effects, strong magnetic fields, instrumental broadening, or other phenomena.

We have determined the number density of particles of regions with spectral line formation in the atmosphere of the Sun and in the atmospheres of solar type stars. We used the fwhm of the spectral lines, the effective temperatures of the stars, and a few basic atomic parameters to infer the number density of particles. We found that the number density of particles in regions where the Balmer lines are being formed decreases with increases in quantum number of the transition. The number density of particles in regions where the  $H\alpha$  absorption line is being formed is three times higher than the number density of particles in regions where the  $H\delta$  line is being formed. Possibly these results were already expected; however, in this work we have used a new method that allows us to quantify directly the changes in the physical conditions of the stellar atmospheres. We also found that the number density of particles in regions where the magnesium triplet absorption lines are being formed seems to change as a function of the stellar metallicity. The magnesium spectral lines have been employed as tracers of the chemical abundances of the stars; our results seem to follow a similar behavior. It is important to point out that the equation employed in this study does not take into account broadening of the spectral lines produced by stellar rotation, stellar winds, or other phenomena. Thus, results obtained for the stars HD 126868, HD 159181, HD 209750, and HD 221170 should be taken with caution.

We have shown that the number density of particles of the regions with spectral line formation estimated in this work is in agreement with the physical properties of the solar atmosphere model. According to the atmosphere model, the  $H\alpha$  line is being formed in the outer parts of the atmosphere where many more hydrogen atoms are not ionized; therefore, most of these atoms can carry out the transition from state  $n = 2$  to the state  $n = 3$ ; then the densities of particles of the region where the  $H\alpha$  absorption line is being formed obtained with both methods are very similar. On the other hand, the fwhm of the  $H\delta$  spectroscopic line allowed us to infer a number density of particles of the regions where the line is being formed that is lower than the density estimated with the atmosphere model. Even if this result seems to be wrong, it is fine, because the  $H\delta$  line is being formed at deeper regions, so the temperature is higher, and the number of particles performing the transition from state  $n = 2$  to the state  $n = 6$  is lower. Thus the results presented in this work are in agreement with the expected physical properties in the atmospheres of G2 spectral type stars.

The full width at half maximum of an absorption line is a useful tool to study the physical conditions of the region where the spectral line is being formed. It allows us to infer the physical properties of the plasma in the atmosphere of a star that the atmosphere model cannot do.

This research has made use of the SIMBAD database, operated at CDS, Strasbourg, France.

## REFERENCES

1. R. Kurucz, ATLAS9 Stellar Atmosphere Programs and 2 km/s grid. Kurucz CD-ROM No. 13. Cambridge, Mass.: Smithsonian Astrophysical Observatory, 1993a, 13.
2. R. Kurucz, SYNTHE Spectrum Synthesis Programs and Line Data. Kurucz CD-ROM No. 18. Cambridge, Mass.: Smithsonian Astrophysical Observatory, 1993b, 18.
3. I. Hubeny and T. Lanz, *Astrophys. J.*, **439**, 875, 1995.
4. O. Cardona, *Astrophysics*, **54**, 75, 2011a.
5. O. Cardona, A. Flores, and L. H. Rodríguez-Merino, *Astrophysics*, **54**, 538, 2011b.
6. P. Prugniel and C. Soubiran, *Astron. Astrophys.*, **369**, 1048, 2001.
7. P. Prugniel, C. Soubiran, M. Koleva, and D. Le Borgne, arXiv:astro-ph/0703658, 2007.
8. R. L. Kurucz, I. Furenlid, J. Brault, and L. Testerman, National Solar Observatory Atlas, Sunspot, New Mexico: National Solar Observatory, 1984.
9. R. Glebocki and P. Gnacinski, VizieR Online Data Catalog, 3244, 2005.
10. G. Worthey and D. L. Ottaviani, *Astrophys. J. Suppl. Ser.*, **111**, 377, 1997.
11. G. Worthey, S. M. Faber, J. J. Gonzalez, and D. Burstein, *Astrophys. J. Suppl. Ser.*, **94**, 687, 1994.
12. L. Crivellari, O. Cardona, and E. Simonneau, *Astrophysics*, **45**, 480, 2002.